DOI: 10.1002/ejic.201100306

Solvothermal Treatment of Triangular Molybdenum(IV) Oxo Species – A New Approach for the Synthesis of New Molybdenum Oxo Clusters

Jun Zhao[a] and Li Xu*[a]

Dedicated to Professor John D. Corbett on the occasion of his 85th birthday

Keywords: Molybdenum / Cluster compounds / Metal–metal interactions / Mixed-valent compounds / Solvothermal synthesis

An unprecedented solvothermal treatment of triangular molybdenum oxo clusters $K_2[Mo_3O_4(Hnta)_3]$ (**1**, nta = nitrilotriacetate) and $H_2bipy[Mo_3O_4(C_2O_4)_3(H_2O)_3]$ (**2**, bipy = 4,4′-bipyridine) was successfully established to prepare a series of new oligonuclear Mo(IV–VI) oxo clusters **3**–**5**. Hydrothermal treatment of **1** in aqueous solution produced the hexanuclear cluster $[Mo^{IV}_6O_{10}(bpy)_4(Hnta)_2]\cdot 10H_2O$ (**3**, bpy = 2,2′-bipyridine). Solvothermal oxidation of **2** was performed in pyridine (py) to yield the unprecedented decanuclear mixed-valent oxo cluster $[Mo^{IV}_6Mo^{VI}_4O_{24}py_8]\cdot py$ (**4**). The further oxidized product $[Mo^{V}_8Mo^{VI}_2O_{26}py_8]\cdot 2py$ (**5**) was obtained from a reaction at a higher temperature and for a longer duration. Clusters **3**–**5** have been characterized by X-ray crystallography, elemental analysis, and UV/VIS and IR spectroscopy.

Introduction

The synthesis of oligonuclear meal clusters has received extensive interest because of their intriguing metal–metal bonding and structural diversity.[1] Of special interest are molybdenum oxo cluster species because of their relevance to the aqueous and biochemistry of molybdenum,[2] interesting structural topologies,[3–17] catalytic,[18] electrochemical,[2,19] and kinetic[20] properties. Mo^{IV} oxo clusters are dominated by three major types of triangular oxo species: $[Mo_3O_4L_9]$,[3] $[Mo_3O_2(O_2CR)_6L_3]$,[4] and $[Mo_3O(OR)_{10}]$.[5] These trinuclear Mo^{IV} cluster compounds are electron precise in that they have the six electrons needed to establish three Mo–Mo bonds. For the +5 oxidation state, dinuclear oxo complexes such as $[Mo_2O_4]^{2+}$ derivatives are the dominant species with two electrons to form one Mo–Mo bond.[6] Conversely, Mo^{VI} has been known to form polyoxoanions without Mo–Mo bonding.[1b,7] In contrast to the well established oxo chemistry of single-valent Mo^{IV}, Mo^{V}, and Mo^{VI} compounds, their mixed-valent oxo chemistry,[8–16] especially that of Mo^{IV}–Mo^{VI},[17] is far less investigated, and there have been few new structural types of oxomolybdenum clusters reported in recent years. This situation may result from the fact that only simple mononuclear starting materials and conventional reactions under ambient pressure have been employed, which usually leads to the formation of oxomolybdenum clusters of a single oxidation state. Mixed-valent oxomolybdenum clusters can be viewed as a bridge between low-valent Mo–Mo bonded oxo clusters and polyoxoanions and are expected to exhibit unique structural features. We have previously shown that heating a mixture of $[Mo^{IV}_3O_2(O_2CR)_6L_3]$ and $M(CO)_x$ in carboxylic anhydride gives octanuclear $[Mo^{IV}_3O_4M^{III}M^{III}Mo^{IV}_3O_4]$[21] clusters (M = Cr, Mo, W, Fe), which exhibit zero-field absorption characteristic of oxide superconductors.[22] In this work, we report a new approach for the synthesis of molybdenum oxo clusters, namely the solvothermal treatment of triangular Mo^{IV} oxo clusters, which produced a series of new Mo_6^{IV} (**3**), mixed-valent $Mo_6^{IV}Mo_4^{VI}$ (**4**), and $Mo_8^{V}Mo_2^{VI}$ compounds (**5**) under different reaction conditions.

Results and Discussion

The syntheses of the oligonuclear clusters **3**–**5** are shown in Scheme 1. It is important to note that protonated bipy (H_2bipy^{2+}) as a counter cation can greatly enhance the solubility of the resulting triangular $[Mo_3O_4]$ clusters (**2**) in organic solvents such as pyridine, which is essential to the subsequent solvothermal reactions of the trinuclear oxo clusters in organic solvents. Solvothermal synthesis was used successfully to prepare coordination polymers by self-assembly of metal ions and multifunctional organic ligands, which have been far less investigated with metal clusters as precursors.[21–22] The reactions of $Na[M^{IV}_3O_2(O_2CEt)_9]$ (M_3

[a] State Key Laboratory of Structural Chemistry, Fujian Institute of Research on the Structure of Matter, Chinese Academy of Sciences,
Fuzhou, Fujian 350002, China
Fax: +86-591-83705045
E-mail: xli@fjirsm.ac.cn

= Mo_3, MoW_2, W_3) with $M'(CO)_x$ (M′ = Fe, Cr, Mo) on heating with carboxylic anhydride under ambient pressure have been previously reported to produce the hetero-octametallic clusters $Na_2[M'^{III}M^{IV}{}_3O_4(O_2CEt)_8]_2$.[21–22] In these reactions with the reducing reagents $M'(CO)_6$, only the structural transformation from the bioxo-capped $[M_3O_2]^{8+}$ to the imcomplete cuboid $[M_3O_4]^{4+}$ occurs without a change in oxidation state.

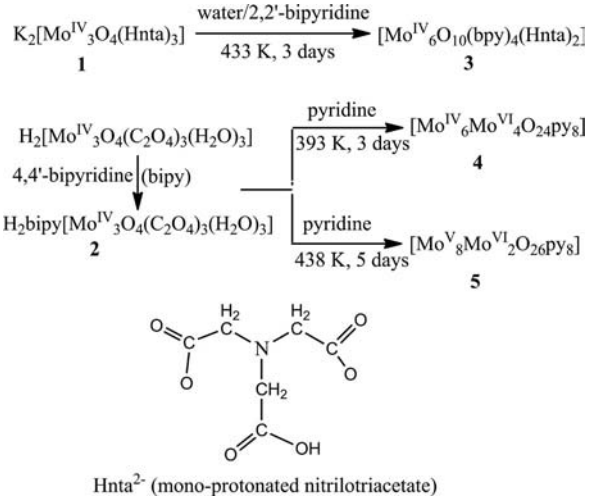

Scheme 1. Solvothermal syntheses of the oligonuclear oxo clusters **3**–**5**.

Scheme 1 shows the hydrothermal treatment of **1**, which is insoluble in organic solvents, in aqueous solution in the presence of bpy, which led to the replacement of two of three Hnta ligands with four bpy and two μ_2-O ligands without a change in oxidation state in the resulting hexanuclear cluster **3**. This recognizes that Mo^{IV} is a stable oxidation state in aqueous solution.[2,3] However, its stability was markedly reduced when the coordinating water molecules were substitutd by organic ligands such as cyanide[2,3] and unprotonized organic solvents were employed.[2,19] With these concerns in mind, the solvothermal air-oxidation of **2** in pyridine, which was believed to substitute the coordinating oxygen atoms as well, was successfully established to synthesize the decanuclear Mo^{IV}–Mo^{VI} cluster **4**, wherein the partial oxidation of Mo^{IV} to Mo^{VI} occurred. At an enhanced reaction temperature and for a longer duration, the further oxidized Mo^{V}–Mo^{VI} **5** was obtained. The UV/Vis absorption spectrum of **4** in pyridine displayed a peak at 520 nm similar to that (505 nm) of **1** (Figure S1, Supporting Information), indicating that the cluster unit also exists in solution but the electronic structure is significantly affected by the bridging $[MoO_4]^{2-}$ (to be discussed later). Cluster **5** has a shoulder peak at about 289 nm, similar to that of $Na_2[Mo_2O_4EDTA]$ (298 nm), suggesting that the decanuclear cluster **5** comprising four $[Mo^{V}{}_2O_4]$ units also exists in solution.

X-ray structural analysis of **2** reveals the triangular unit $[Mo_3O_4(C_2O_4)_3(H_2O)_3]^{2-}$, which is charge balanced by the H_2bipy^{2+} ligand. The structure of $[Mo_3O_4(C_2O_4)_3(H_2O)_3]^{2-}$ (Figure 1) consists of the well known incomplete cuboidal $[Mo_3O_4]^{4+}$ core that is supported by $C_2O_4^{2-}$ and H_2O ligands to complete the octahedral coordination of each Mo atom (not counting the Mo–Mo bond). The Mo–Mo and Mo–O bonds are not significantly different from reported values.[2a] Interestingly, there are extensive hydrogen bonds between the three coordinating H_2O and three $C_2O_4^{2-}$ ligands (O18–H···O6 2.68, O17–H···O7 2.77, O19–H···O10 2.71, O18–H···O16 2.63 Å), which interconnect the trinuclear cluster dianions into a 3D porous supramolecular framework with square channels (10.0 × 9.0 Å) occupied by H_2bipy^{2+} countercations (Figure 2), presumably responsible for the easy formation of crystals. The H_2bipy^{2+} is hydrogen bonded to two $C_2O_4^{2-}$ units, indicated by short N1···H^+···O distances (N1···H^+···O12 2.67, N2···H^+···O8 2.80 Å). Thermogravimetric analysis (TGA) of **2** (Figure 3) shows the first weight loss of 6.0% before 200 °C caused by the release of solvent water molecules (calculated 6.1%). Bipy is lost before 320 °C, contributing to the 17.5% weight loss (calculated 17.7%). The subsequent weight loss should result from the decomposition of oxalate and coordinating water, which should contribute 36% weight loss. However, the

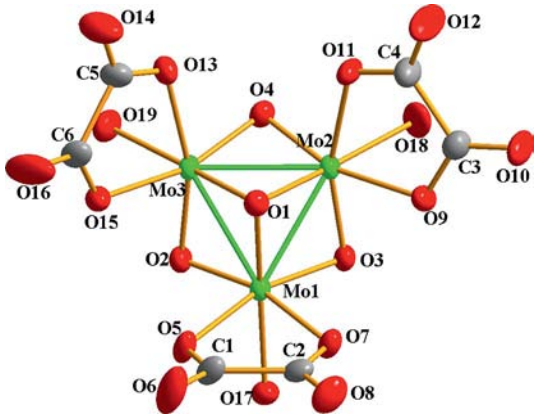

Figure 1. Molecular structure of **2** with 50% probability thermal ellipsoids.

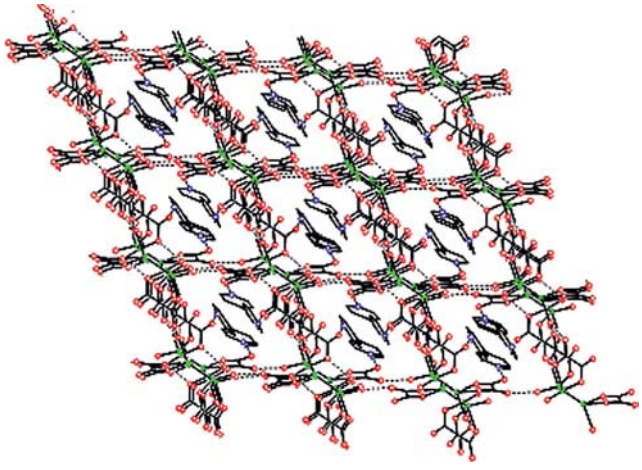

Figure 2. 3D microporous supramolecular structure of **2** with the channels (10.0 × 9.0 Å) filled by H_2bipy^{2+}.

weight loss of 22% before 600 °C reveals that the oxalate carbon atoms remain in the residual product. This is supported by the fact that only 36% of **2** was left after 700 °C, which was more likely to be MoC (calculated 36.7%) than MoO_2 (calculated 43%).

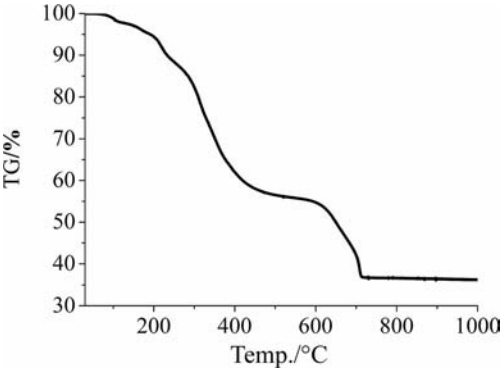

Figure 3. TGA curve of **2**.

Cluster **3** consists of the hexanuclear cluster cation $[Mo^{IV}_6O_{10}]^{4+}$ charge balanced by two $Hnta^{2-}$ anions as well as four bpy ligands. The centrosymmetric $[Mo^{IV}_6O_{10}]^{4+}$ unit can be described as two incomplete cuboid $[Mo_3O_4]^{4+}$ cores doubly bridged by two μ_2-O atoms (O5) into a cyclic structure (Figure 4) somewhat similar to that of the cyclic $[Mo_3O_4MMO_4Mo_3]^{8+}$ clusters.[21–22] The assignment of O5 as O^{2-}, rather than OH^-, is based both on the short Mo–μ_2-O5 bonds [Mo1–O5 1.907(3), Mo2–O5 1.898(3) Å] similar to the Mo–O_b bond distances in the $[Mo_3O_4]^{4+}$ core [1.900(5)–1.914(5) Å in **2**] and the absence of hydrogen atoms around O5. This assignment also agrees with the charge balance requirement mentioned above. The strong Mo–μ_2-O5 interactions exhibit a remarkable *trans* effect revealed by the Mo1–O4 [1.998(3) Å] and Mo2–O3 [2.005(3) Å] distances, which are considerably longer than those of Mo1–O2 [1.934(3) Å] and Mo2–O2 [1.929(3) Å]. The Mo–Mo bonds in **3** [2.502(2), 2.546(2), 2.547(2) Å] are longer than those of **2** [2.4756(8), 2.4836(8), 2.4902(8) Å], indicating that the Mo–Mo bonding of **3** is significantly weakened, presumably caused by the delocalization of the electrons of the Mo–Mo bonding orbitals over the Mo–O5 bonding orbitals of partial double bonding. Four bpy and two $Hnta^{2-}$ ligands complete the octahedral coordination around each Mo^{IV} atom (Figure 5). Two pairs of bpy ligands, with a dihedral angle of 5.47° and a distance of 3.68 Å, show significant π–π stacking interactions, which further stabilize the hexanuclear structure of **3**. There are extensive hydrogen bonds between the carboxylate oxygen atoms and solvent water molecules, which constitute a 3D supramolecular structure (Figure S3, Supporting Information). It is notable that the O10···O1w hydrogen bond (2.543 Å) is unusually short, indicative of the presence of a proton between them, in agreement with the longest protonated C26–O10 bond [1.310(6) Å].

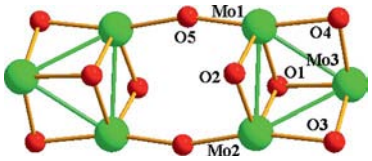

Figure 4. Hexanuclear structure of **3**.

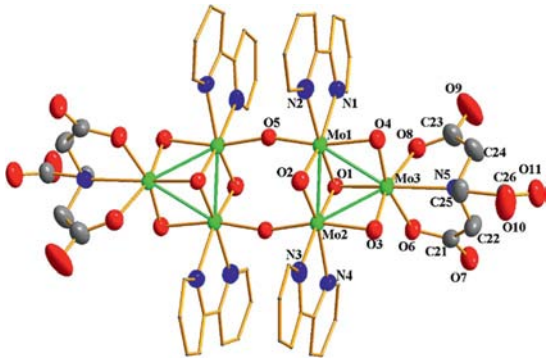

Figure 5. ORTEP drawing of **3** with 50% probability thermal ellipsoids.

The neutral, decanuclear cluster **4** may best be formulated as $[Mo^{IV}_3O_4py_3]_2[Mo^{VI}O_4py_{0.5}]_4$·py, where the two incomplete cuboid $[Mo_3O_4]^{4+}$ cores are charge balanced by four $[MoO_4]^{2-}$ dianions. Figure 6 shows the centrosymmetric structure of **4**. The decanuclear oxo cluster core can be described as two incomplete cuboid $[Mo_3O_4]^{4+}$ units that are quadruply bridged by the four tricoordinated μ_3-MoO_4^{2-} units into a cage structure. Such a $[Mo_3O_4]_2(\mu_3\text{-}MoO_4)_4$ structural feature determines the coexistence of Mo^{IV} and Mo^{VI} rather than comproportionating to Mo^V, which forms only one Mo–Mo bond.[6] Unlike **3**, which has a side-by-side arrangement of the two $[Mo_3O_4]^{4+}$ cores, **4** shows a head-to-head placement of the two $[Mo_3O_4]^{4+}$ units as a consequence of the replacement of μ_2-O in **3** by μ_3-MoO_4^{2-} in **4**. Each MoO_4^{2-} unit uses three oxygen atoms to link two $[Mo_3O_4]^{4+}$ units together, including two spanning one Mo–Mo edge of one $[Mo_3O_4]^{4+}$ unit and the third singly bonded to the Mo^{IV} atom in the other $[Mo_3O_4]^{4+}$ unit. The three Mo–Mo distances are 2.5078(10), 2.5340(10), and 2.5042(11) Å, with the average value [2.5153(11) Å] lying between those of **2** [2.4831(8) Å] and **3** [2.532(2) Å], indicating that the Mo–Mo bonding is less weakened by μ_3-MoO_4^{2-} than μ_2-O. The Mo^{VI}–O_b (O5–O10) bonds [1.787(5)–1.827(6) Å] are markedly shorter than $[Mo^{IV}_3]$–O_b [2.060(6)–2.158(6) Å] as expected for the double and dative bonds of $[Mo^{VI}O_4]^{2-}$ and $[Mo^{IV}_3]$–O_b, respectively. It is notable that these Mo^{VI}–O_b bonds are significantly longer than the free Mo^{VI}–O_t bonds [Mo4–O11 1.704(6), Mo5–O12 1.708(6) Å], indicating that the Mo^{VI}=O double bonding of the bridging molybdate is significantly weakened by coordination to the $[Mo_3]$ clusters. The $[Mo^{IV}_3]$–O_b (MoO_4^{2-}) [2.060(6)–2.158(6) Å] bonds in **4** are significantly longer than the corresponding $[Mo^{IV}_3]_2$–

(μ-O) bonds [1.907(3), 1.898(3) Å] in **3** and exhibit less of a *trans* effect as indicated by the almost unchanged bond lengths [1.912(6)–1.946(6) Å] in the $[Mo_3O_4]^{4+}$ units of **4**.

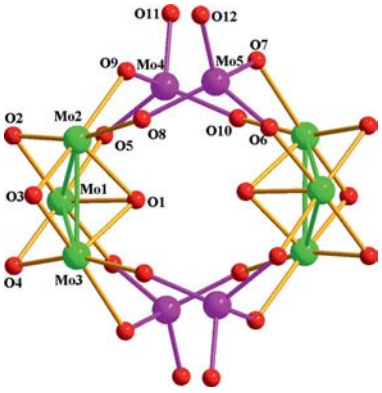

Figure 6. Decanuclear structure of **4** (Mo^{IV} green, Mo^{VI} purple).

Figure 7 shows that there are eight peripheral py ligands surrounding the $Mo_{10}O_{24}$ cluster core. Six of these are coordinated to the $[Mo_3O_4]^{4+}$ units in positions *trans* to the capping oxygen atoms to complete the octahedral coordination of each Mo (not couting the Mo–Mo bonds). The Mo–N bond lengths are 2.240(11), 2.230(13), and 2.209(11) Å. The remaining two py ligands are bonded to only two of the four μ_3-MoO_4^{2-} units as a consequence of steric hindrance. The Mo^{VI}–N distances [Mo4–N4 2.410(7) Å] are significantly longer than the py–Mo_3O_4 distances [2.215(7)–2.238(8) Å] because of the stronger *trans* effect of the shorter Mo4–O9 bond [1.805(5) vs. 2.020(8)–2.041(5) Å of py–{Mo_3O_4}]. The additional py ligand does not affect the Mo4–O bonds, which are similar to those around Mo5, but has a significant influence on the coordination geometry of the central Mo4 atom. The sum of the angles between O5, O10, and O11 and Mo4 [349.9(5)°] is larger than that for Mo5 [< 338.1(5)°] because of the apical coordination of the py ligand. The N4–Mo4–O9 angle [172.1(4)°] is almost linear and the coordination geometry of Mo4 can be described as trigonal bipyramid with the axial positions occupied by N4 and O9 and the equatorial positions taken up by O5, O10, and O11.

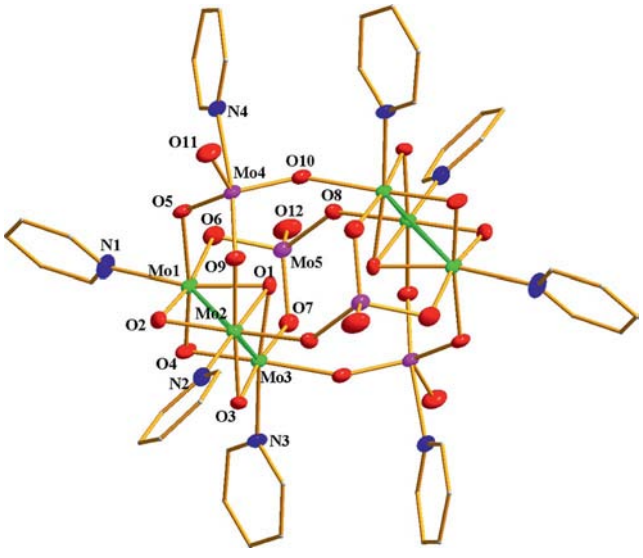

Figure 7. ORTEP drawing of **4** with 50% probability thermal ellipsoids (Mo^{IV} green, Mo^{VI} purple).

Extensive C–H···O and C–H···N hydrogen bonds interconnect the decanuclear cluster **4** into a 3D supramolecular porous structure (Figure S4, Supporting Information) with the channels templated by pyridine solvent molecules. It is notable that these pyridine molecules are parallel to each other with a separation distances of 3.81 Å and a dihedral angle of 7.88°, showing π–π stacking interactions.

Similar to **3** and **4**, compound **5** (Figure 8) has a crystallographically-imposed symmetry of invension center. It is best described as a dicapped cuboid structure with the eight cuboidal vertices occupied by Mo^V centers from the four interconnected $[Mo^V_2O_4]$ units and the two capping sites taken up by Mo^{VI} centers (Mo3) from the two $Mo^{VI}O_5$ moieties. The existence of four $[Mo_2O_4]$ units allows Mo^V with one Mo–Mo bond to exist in **5** rather than Mo^{IV}, which forms two Mo–Mo bonds in a triangular Mo_3 structure.[3–5] The Mo–Mo single bonds [Mo1–Mo2 2.5971(9), Mo4–Mo5 2.5690(9) Å], similar to those in $Na_2[Mo^V_2O_4EDTA]$ [2.550(1) Å],[7c] confirm the presence of Mo–Mo bonded $[Mo^V_2O_4]$ units as expected for an oxidation state of +5. Half of the bridging oxygen atoms (O3, O10) of $[Mo^V_2O_4]$ are weakly coordinated to one neighboring $[Mo^V_2O_4]$ unit [Mo5–O3 2.307(5), Mo1–O10 2.239(5) Å] in positions *trans* to Mo=O to interconnect the four $[Mo^V_2O_4]$ moieties into a cubane-like structure with parallel Mo–Mo bonds. The cuboidal $[Mo^V_2O_4]_4$ units are further linked by two μ_3-O (O5, O9) and two μ_2-O (O6, O7) from the capping μ_4-$Mo^{VI}O_5$ unit with the five oxygen atoms in a square pyramidal arrangement. It is notable that the bond lengths in $Mo^{VI}O_5$ are highly dependent on the coordination number of the oxygen atoms. The Mo^{VI}–μ_3-O [Mo3–O5 2.022(5), Mo3–O9 1.977(5) Å] bonds are markedly longer than the Mo^{VI}–μ_2-O [Mo3–O6 1.863(5), Mo3–O7 1.802(5) Å] and Mo^{VI}=O bonds [Mo3–O8 1.685(5) Å]. Considering the structural evolution from **4** to **5**, we suggest that the further

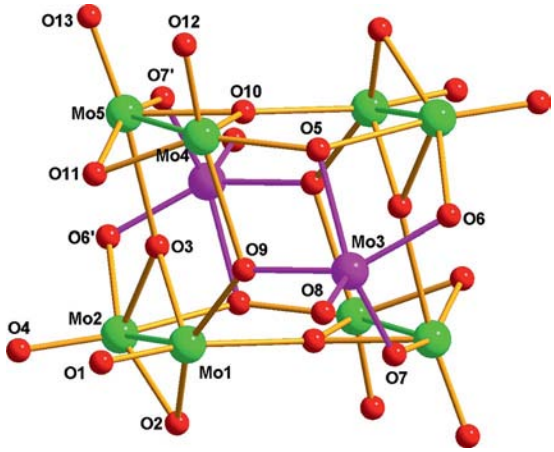

Figure 8. Decanuclear structure of **5** (Mo^V green, Mo^{VI} purple).

oxidation occurs at $[Mo^{IV}_3O_4]^{4+}$ of **4**, which is oxidized to the interconnected $[Mo^{V}_2O_4]$ of **5** accompanied by the conversion of the bridging μ_3-MoO_4^{2-} to the capping μ_4-$Mo^{VI}O_5$.

Figure 9 shows the eight py ligands coordinated to the four $[Mo_2O_4]$ units in positions *trans* to the μ_3-O (O3, O10) atoms to complete the octahedral coordination of each Mo atom with Mo–N distances [2.227(6)–2.264(6) Å] similar to those in **4**. The decanuclear structure of **5** is further stabilized by extensive C–H···O hydrogen bonds that link the cluster molecules into an extended supramolecular architecture (Figure S5, Supporting Information).

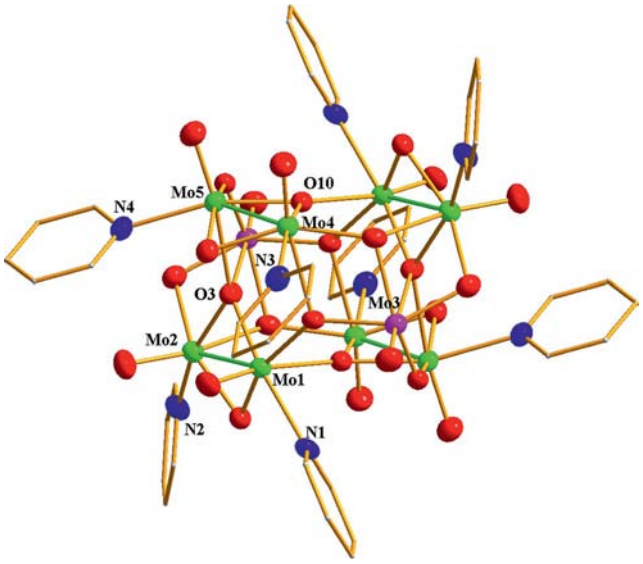

Figure 9. ORTEP drawing of **5** with 50% probability thermal ellipsoids (Mo^{V} green, Mo^{VI} purple).

Conclusions

Solvothermal treatment of triangular molybdenum(IV) oxo cluster compounds was successfully developed to prepare the unprecedented oligonuclear oxomolybdenum clusters $[Mo^{IV}_6O_{10}(bpy)_4(Hnta)_2]$(**3**), $[Mo^{IV}_6Mo^{VI}_4O_{24}py_8]$·py (**4**), and $[Mo^{V}_8Mo^{VI}_2O_{26}py_8]$·2py (**5**). Mo^{IV} shows a stable oxidation state in aqueous solution and thus oxidation has not been observed in the hydrothermal preparation of **3**. The reduced stability of Mo^{IV} in organic solvents leads to the formation of the mixed-valent oxo clusters **4** and **5** depending on reaction temperature and duration. Such solvothermal treatment of known low-valent molybdenum oxo clusters provides a new approach for the synthesis of new types of molybdenum oxo clusters.

Experimental Section

Methods and Materials: $[Mo_3O_4(H_2O)_9]^{4+}$ and $H_2[Mo_3O_4(C_2O_4)_3(H_2O)_3]$ were prepared according to the published procedure.[3c] All other chemicals were obtained from commercial sources and used without further purification. Elemental analyses were performed with a Vario EL III elemental analyzer. IR spectra were recorded with a Magna 750 FTIR spectrometer photometer as KBr pellets in the 4000–400 cm^{-1} region. UV/VIS spectra were recorded as pyridine solutions with a PerkinElmer lambda-900. TGA data were recorded with a Netzsch STA449C.

$K_2[Mo_3O_4(Hnta)_3]\cdot 3H_2O$ (1): H_3nta (0.40 g, 2 mmol) was added to an aqueous solution of $[Mo_3O_4(H_2O)_9]^{4+}$ (ca. 7.5 mmol) (30 mL). The pH of the resulting solution was adjusted to 7 by the addition of KOH (1 M). The filtered solution was evaporated in air to give red crystals of **1** in 50% yield (based on H_3nta). $C_{16}H_{22}Mo_3N_2O_{22}$ (882.17): calcd. C 20.60, H 2.40, N 4.00; found C 20.16, H 2.68, N 4.25. IR (KBr): $\tilde{\nu}$ = 3662 (m), 2949 (m), 1686 (s), 1446 (s), 1334 (s), 1222 (vs), 1110 (m), 920 (m), 799 (m) cm^{-1}.

H_2bipy$[Mo_3O_4(C_2O_4)_3(H_2O)_3]\cdot 3H_2O$ (2): Bipy (0.313 g, 2 mmol) in a mixture of EtOH and H_2O was added to an aqueous solution of $H_2[Mo_3O_4(C_2O_4)_3(H_2O)_3]$ (ca. 2.5 mmol) (10 mL). The mixture was eluted from an ion-exchange column with a 0.5 M solution of oxalic acid, and the resulting solution was exposed to air for several days to give red crystals of **2** (1.0 g, 57%). $C_{16}H_{22}Mo_3N_2O_{22}$ (882.17): calcd. C 21.77, H 2.49, N 3.18; found C 21.88, H 2.52, N 3.37. IR (KBr): $\tilde{\nu}$ = 3213 (m), 3090 (s), 1707 (s), 1678 (s), 1596 (s), 1488 (m), 1407 (s), 1261 (m), 1201 (m 958 w), 792 (s), 761 (m), 723 (m), 480 (s) cm^{-1}.

$[Mo^{IV}_6O_{10}(bpy)_4(Hnta)_2]$ (3): A mixture of **1** (0.5 g, 0.5 mmol), distilled water (15 mL), and bpy (0.3 g, 0.2 mmol) was sealed in a 20 mL stainless steel reactor with a Teflon® liner and heated at 433 K for 3 d. The reactor was cooled to room temperature at a rate of 0.5 K h^{-1} to give dark red crystals of **3** in about 20% yield (based on bpy). $C_{25}H_{45}Mo_{10}N_9O_{24}$ (1815.08): calcd. C 32.55, H 3.47, N 7.30; found C 33.16, H 3.34, N 7.29. IR (KBr): $\tilde{\nu}$ = 3371 (m), 3113 (m), 3079 (m), 2521 (m), 1721 (m), 1627 (s), 1599 (s), 1494 (m), 1066 (s), 1473 (m), 1445 (m), 1381 (m), 1235 (m), 1031 (m), 922 (m), 794 (s), 737 (s), 640 (s), 693 (m) cm^{-1}.

$[Mo^{IV}_6Mo^{VI}_4O_{24}py_8]\cdot$py (4): A mixture of **2** (0.44 g, 0.5 mmol) and pyridine (15 mL) was sealed in a 20 mL stainless steel reactor with a Teflon® liner and heated at 393 K for 4 d. The reactor was cooled to room temperature at a rate of 5 K h^{-1} to give dark red crystals of **4** (0.30 g, 60%). $C_{25}H_{45}Mo_{10}N_9O_{24}$ (1815.08): calcd. C 26.28, H 2.19, N 6.13; found C 26.20, H 2.21, N 6.16. IR (KBr): $\tilde{\nu}$ = 3367 (m), 3059 (m), 1701 (m), 1679 (m), 1636 (m), 1604 (s), 1484 (s), 1448 (s), 1355 (m), 1216 (s), 1146 (m), 1067 (s), 1067 (s), 1045 (s), 1014 (m), 939 (s), 919 (s), 847 (s), 763 (s), 706 (s), 691 (s), 627 (m), 507 (m), 497 (m), 442 (s) cm^{-1}.

$[Mo^{V}_8Mo^{VI}_2O_{26}py_8]\cdot$2py (5): Cluster **5** was obtained under conditions similar to those desribed for **4**, but with enhanced temperature (438 K) and prolonged reaction time (ca. 5 d). A mixture of **1** (0.44 g, 0.5 mmol) and pyridine (15 mL) was sealed in a 20 mL stainless steel reactor with a Teflon® liner and heated at 438 K for 5 d. The reactor was cooled to room temperature at a rate of 5 K h^{-1} to give red crystals of **5** (0.16 g, 20%). $C_{50}H_{50}Mo_{10}N_{10}O_{26}$ (2166.40): calcd. C 27.72, H 2.32, N 6.46; found C 27.63, H 2.31, N 6.35. IR (KBr): $\tilde{\nu}$ = 3428 (m), 3106 (m), 3059 (m), 2346 (m), 1679 (m), 1603 (s), 1448 (s), 1215 (s), 1066 (s), 1045 (m), 919 (m), 846 (s), 820 (s), 764 (s), 691 (s), 640 (s), 442 (m) cm^{-1}.

X-ray Crystallographic Study: Suitable single crystals of **2**–**5** were mounted on a Siemens Smart CCD diffractometer equipped with a graphite-monochromated Mo-K_α radiation (λ = 0.71073 Å) at 293 K. All structures were solved by the direct methods and refined by full-matrix least-squares fitting on F^2 by SHELXTL-97.[23] All non-hydrogen atoms were refined with anisotropic thermal param-

Table 1. Crystallographic data for **2**–**5**.

	2	**3**	**4**	**5**
Formula	$C_{16}H_{22}Mo_3N_2O_{22}$	$C_{52}H_{68}Mo_6N_{10}O_{32}$	$C_{45}H_{45}Mo_{10}N_9O_{24}$	$C_{50}H_{50}N_{10}Mo_{10}O_{26}$
M	882.18	1920.80	2055.30	2166.40
Crystal system	triclinic	triclinic	monoclinic	triclinic
Space group	$P\bar{1}$	$P\bar{1}$	$C2/c$	$P\bar{1}$
a [Å]	8.9060(2)	10.552(8)	26.5164(3)	11.7720(2)
b [Å]	10.0506(2)	12.655(11)	11.1943(2)	12.0175(5)
c [Å]	16.8584(4)	14.639(12)	22.3295(3)	13.2141(4)
α [°]	101.1140(10)	72.89(3)	90	88.5956(13)
β [°]	97.3780(10)	70.12(4)	115.4900(10)	72.6549(11)
γ [°]	114.7000(10)	70.04(3)	90	67.7574(8)
Volume [Å^3]	1307.75(5)	1692(2)	5982.94(15)	1643.33(9)
Z	2	2	4	1
$d_{calcd.}$ [g/cm^3]	2.240	1.885	2.282	2.189
μ [cm^{-1}]	1.522	1l174	2.106	1.926
$F(000)$	868	958	3960	1048
Crystal size [mm]	$0.50 \times 0.06 \times 0.04$	$0.60 \times 0.40 \times 0.04$	$0.52 \times 0.34 \times 0.22$	$0.14 \times 0.08 \times 0.05$
Data/restraint/parameters	4464/0/388	7628/0/460	5105/0/398	7319/0/433
Reflections collected	6628	12899	9742	12614
Unique reflections	4464	7628	5105	7319
Goodness of fit	1.022	1.007	1.010	1.104
R_1 [$I > 2\sigma(I)$]	0.0660	0.0479	0.0753	0.0593
R_2 [$I > 2\sigma(I)$]	0.1158	0.0621	0.1503	0.1291
R_1 (all data)	0.0761	0.1175	0.0922	0.0886
R_2 (all data)	0.1185	0.1314	0.1592	0.1495
Residuals [e Å^{-3}]	0.871, –0.829	1.589, –0.985	2.098, –0.971	1.301, –1.050

eters. Hydrogen atoms were located at geometrically calculated positions and refined as riding on their parent atom. Crystallographic data and structural refinements for **2**–**5** are summarized in Table 1.

CCDC-606847 (for **2**), -818311 (for **3**), -606848 (for **4**), and -606849 (for **5**) contain the supplementary crystallograplic data for this paper. These data can be obtained free of charge from The Cambridge Crystallographic Data Centre via www.ccdc.cam.ac.uk/data_request/cif.

Supporting Information (see footnote on the first page of this article): UV/Vis spectra of **2**, **4**, and **5**, bond valence calculation for **2**–**5**, 3D supramolecular structures of **3**, **4**, and **5**. This material is available free of charge via the internet at http://www.eurjic.org.

Acknowledgments

This work was supported by the Knowledge Innovation Program (grant number KJCX2-EW-H01) of the Chinese Academy of Sciences, the National Natural Science Foundation of China (grant numbers 21073190, 21003125) and the National Science Foundation of Fujian Province (grant numbers 2010J05040 and 2010J01057).

[1] a) J. D. Corbett, *Inorg. Chem.* **2010**, *49*, 13–28; b) A. Muller, F. Peters, M. T. Pope, D. Gatteschi, *Chem. Rev.* **1998**, *98*, 239–271; c) D. T. Richens, *Commun. Inorg. Chem.* **2005**, *26*, 217–232.

[2] D. T. Richens, *The Chemistry of Aqua Ions*, John Wiley & Sons, Chichester, **1997**.

[3] a) A. Bino, F. A. Cotton, Z. Dori, *J. Am. Chem. Soc.* **1978**, *100*, 5252–5253; b) R. K. Murmam, M. E. Shelton, *J. Am. Chem. Soc.* **1980**, *102*, 3984–3985; c) F. A. Cotton, D. O. Marler, W. Schwotzer, *Inorg. Chem.* **1984**, *23*, 3671–3673; d) M. Brorson, A. Hazell, C. J. H. Jaconson, I. Schmidt, J. Villadsen, *Inorg. Chem.* **2000**, *39*, 1346–1350.

[4] a) A. Birnbaum, F. A. Cotton, Z. Dori, P. O. Marler, G. M. Reisner, W. Schwotzer, M. Shia, *Inorg. Chem.* **1983**, *22*, 2723–2726; b) A. Birnbaum, F. A. Cotton, Z. Dori, M. Kapon, *Inorg. Chem.* **1984**, *23*, 1617–1619; c) A. Bino, D. Gibon, *J. Am. Chem. Soc.* **1982**, *104*, 4383–4388.

[5] a) *Early Transition Metal Clusters with p-Donor Ligands* (Ed.: M. H. Chisholm), VCH Publishers, New York, **1995**; b) M. H. Chisholm, C. M. Cock, K. Folting, *J. Am. Chem. Soc.* **1992**, *114*, 2721; c) M. H. Chisholm, K. Folting, *Inorg. Chem.* **1984**, *23*, 1021–1037.

[6] a) R. L. Pecsok, D. T. Sawyer, *J. Am. Chem. Soc.* **1956**, *78*, 5496–5500; b) V. R. Ott, D. S. Swieter, F. A. Schultz, *Inorg. Chem.* **1977**, *16*, 2538–2545; c) H. Kobayashi, I. Tsujikawa, T. Shibahara, *Bull. Chem. Soc. Jpn.* **1983**, *56*, 108–112; d) B. Modec, M. Sala, R. Clerac, *Eur. J. Inorg. Chem.* **2010**, 542–553.

[7] M. T. Pope, A. Muller, *Angew. Chem.* **1991**, *103*, 56; *Angew. Chem. Int. Ed. Engl.* **1991**, *30*, 34–48.

[8] S. C. Liu, X. Sun, J. Zubieta, *J. Am. Chem. Soc.* **1988**, *110*, 3324–3326.

[9] D. L. Long, P. Kogerler, L. J. Farrugia, L. Cronin, *Angew. Chem.* **2003**, *115*, 4312; *Angew. Chem. Int. Ed.* **2003**, *42*, 4180–4183.

[10] W. B. Yang, C. Z. Lu, X. Lin, H. H. Zhuang, *Chem. Commun.* **2000**, 1623–1624.

[11] D.-L. Long, P. Kogerler, L. J. Farrugia, L. Cronin, *Dalton Trans.* **2005**, 1372–1380.

[12] A. Müller, J. Meyer, E. Krickemeyer, C. Beugholt, H. Bögge, F. Peters, M. Schmidtmann, P. Kögerler, M. J. Koop, *Chem. Eur. J.* **1998**, *4*, 1000–1006.

[13] H. K. Chae, W. G. Klemperer, T. A. Marquart, *Coord. Chem. Rev.* **1993**, *128*, 209–224.

[14] C. Limberg, M. Büchner, K. Heinze, O. Walter, *Inorg. Chem.* **1997**, *36*, 872–879.

[15] R. C. Haushalter, F. W. Lai, *Angew. Chem.* **1989**, *101*, 802; *Angew. Chem. Int. Ed. Engl.* **1989**, *28*, 743–746.

[16] a) Q. Chen, S. Liu, J. Zubieta, *Angew. Chem.* **1988**, *100*, 1792; *Angew. Chem. Int. Ed. Engl.* **1988**, *27*, 1724–1725; b) B. Modec, J. V. Brencic, I. Leban, *Inorg. Chem. Commun.* **1998**, *1*, 161–163.

[17] C. le. Roy, F. Y. Pétillon, K. W. Muir, P. Schollhammer, J. Talarmin, *J. Organomet. Chem.* **2006**, *691*, 898–906.
[18] D. A. Ledwith, F. A. Schultz, *J. Am. Chem. Soc.* **1975**, *97*, 6591–6592.
[19] G. Powell, D. T. Richens, *Dalton Trans.* **2006**, 2959–2963.
[20] D. T. Richens, *Chem. Rev.* **2005**, *105*, 1961–2002.
[21] a) L. Xu, H. Liu, J. S. Huang, Q. E. Zhang, *Chem. Eur. J.* **1997**, *3*, 226–231; b) L. Xu, H. Liu, D. Yan, J. S. Huang, Q. E. Zhang, *J. Chem. Soc., Dalton Trans.* **1994**, 2099; c) L. Xu, Z. Li, J. S. Huang, *Inorg. Chem.* **1996**, *35*, 5097–5100.
[22] L. Xu, D. Yan, H. Liu, J. S. Huang, Q. E. Zhang, *J. Chem. Soc., Chem. Commun.* **1993**, 1507–1510.
[23] G. M. Sheldrick, *SHELXL-97*, University of Göttingen, Germany, 1**997**.

Received: March 25, 2011
Published Online: July 19, 2011

